Doped Lanthanum Chromite-refractory Based Composites Sensors for High Temperature Monitoring in Harsh Environments Systems

Javier A. Mena[1], Katarzyna Sabolsky[1], Konstantino Sierros[1], Rowan Barto[1], Nick Voorstad[1], Edward M. Sabolsky[1]

[1]Department of Mechanical and Aerospace Engineering,
West Virginia University, Morgantown, WV 26506, USA

MS&T'23 Presentation October 4th-2023
Advanced Materials for Harsh Environments

WestVirginiaUniversity.

Introduction

- Processes such as energy generation, metals/glass manufacturing, coal gasification and aerospace technology applications require health and process monitoring in harsh-environments.
- **Harsh-environments conditions include:**
  - High temperature (500-1800^{o}C)
  - High pressure (up to 1000 psi)
  - **Corrosive, erosive and reducing environments.**
- **Ability to monitor:**
  - Temperature
  - Structural stability of systems components.

- **US DOE Overall Goal:** Develop health and temperature sensors (and sensor arrays) embedded into refractory compositions.

Objectives of This Work

- To synthesize doped lanthanum oxides perovskites by Sol-Gel method and prepare conductive refractory composites.
- To study the electrical conductivity and Seebeck coefficients of such compositions at temperatures up to 1500 ^{o}C under different working atmospheres (oxidizing, reducing).
- To fabricate surface printed thick-film sensors utilizing these materials and to determine their thermoelectrical response.
- Fabricate sensors embedded into refractory and perform thermoelectrical testing.

Lanthanum Chromite: General Aspects

- High melting point (~2500 °C).
- Chemically stable under oxidative and reducing atmospheres.
- Pure $LaCrO_3$ shows semiconducting behavior with no to low ionic conduction.
- Calcium substitution increase conductivity from 1.0 to 40.0 S·cm at 1000°C (Mori *et al.* 1997)
- Compatibility (thermal expansion coefficients matching) near refractory materials, ~10×10^{-6} $^{o}C^{-1}$.

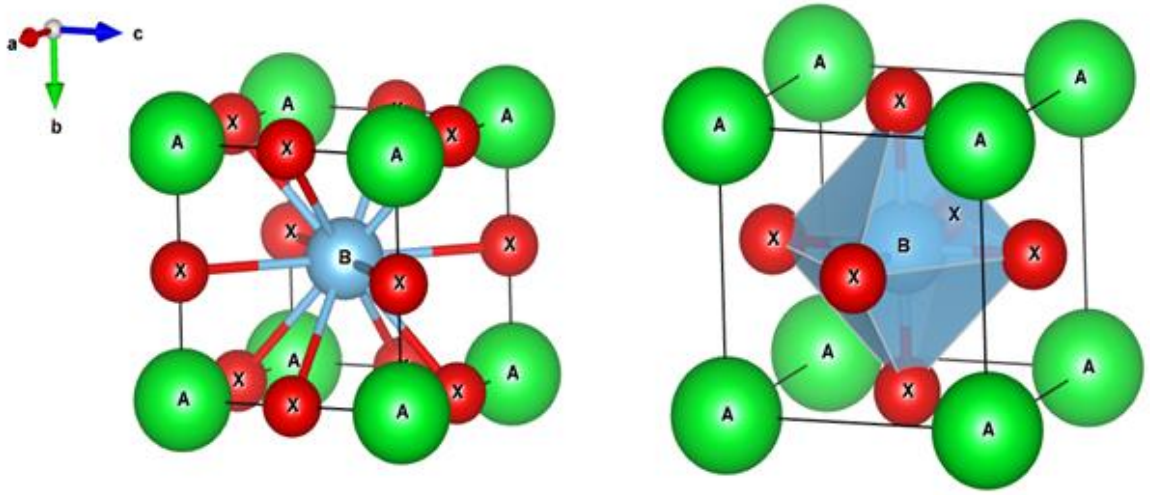

A atom cubic unit cell *B atom cubic unit cell*

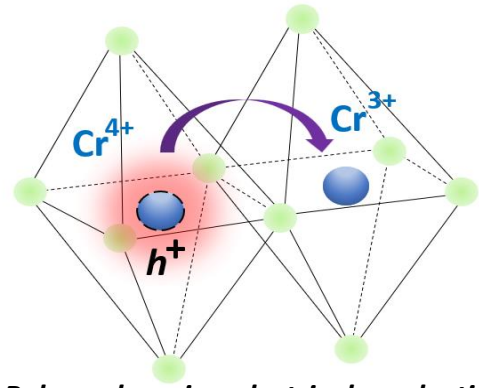

Polaron hopping electrical conduction

Sol Gel Synthesis and Pellet Fabrication

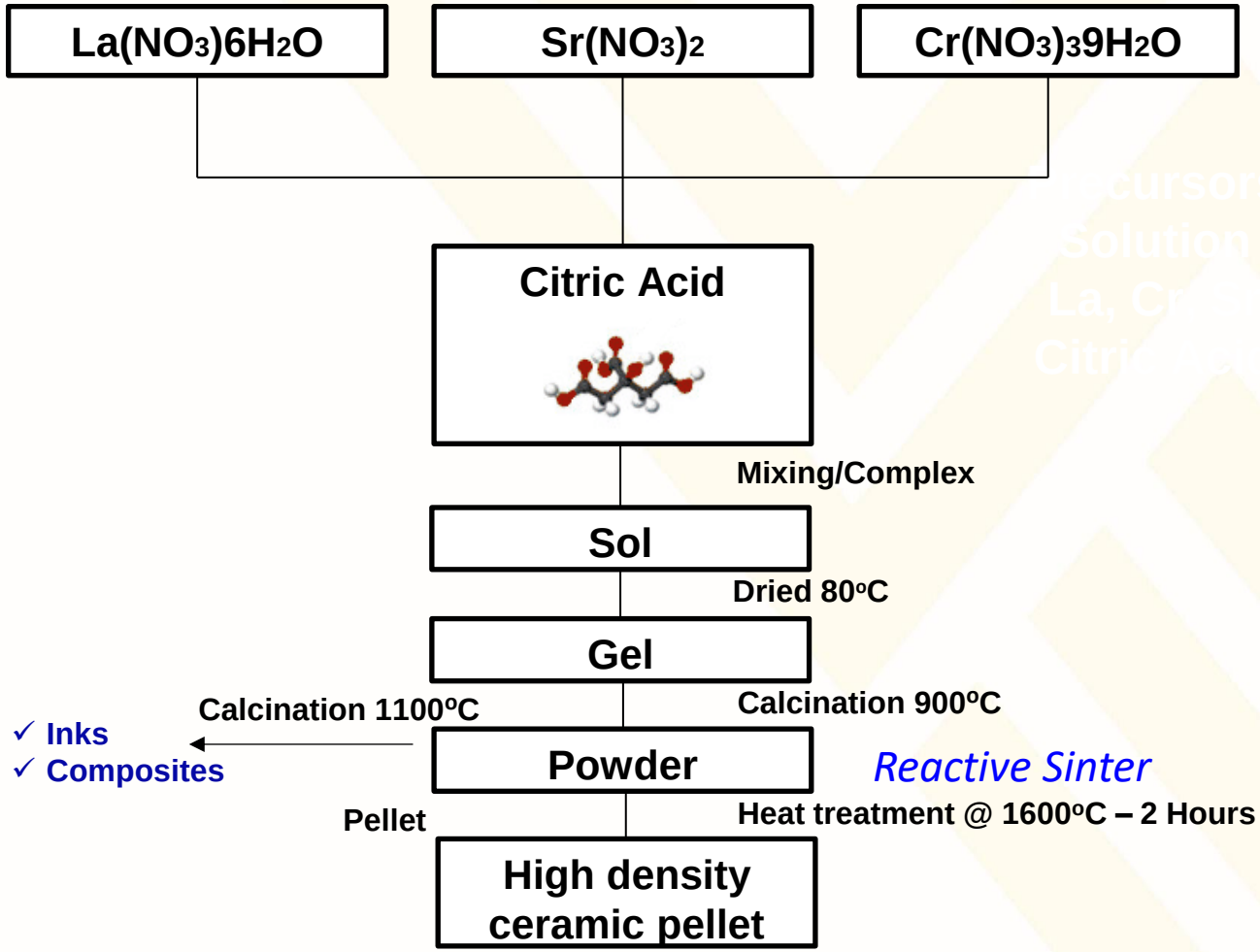

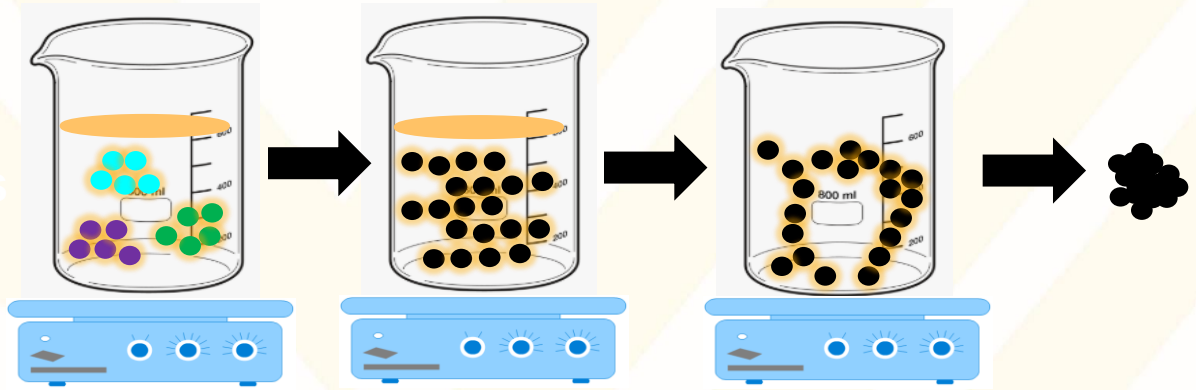

- ✓ Pechini-like process used.
- ✓ High homogenous and adequate sintering.
- ✓ High density (typical in literature <93% density).
- ⊘ Low yields and not easy to scale-up

Compositions Studied:

A-site: $La_{1-x}\mathbf{Sr}_xCrO_3$, $La_{1-x}\mathbf{Ca}_xCrO_3$

(x = 0.1, 0.2, 0.3, 0.4)

B-site: $La_{0.8}Sr_{0.2}Cr_{1-y}\mathbf{Mn}_yO_3$

(y = 0.1, 0.2, 0.3, 0.4)

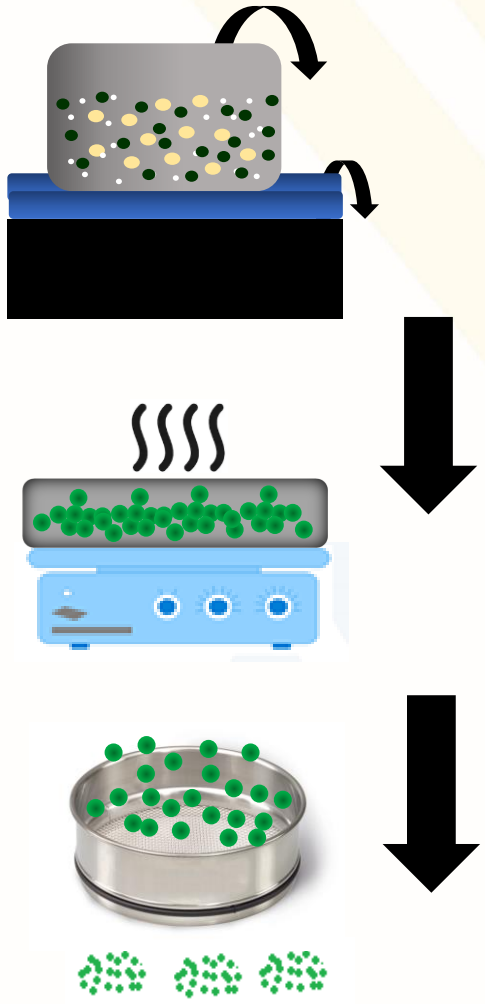

*Pure or 30% Calcium $LaCrO_3$ Powder

Zirconia milling media + Al_2O_3 Powder

Ball milling in isopropanol for 2 h

Zirconia milling media removal

Isopropanol evaporation and composite powder drying at 80 °C

Dried pure/ doped $LaCrO_3$ -Al_2O_3 based composite powders sieving

*The composites were prepared mixing 30% Ca doped $LaCrO_3$ (LCC30) with Al_2O_3 at different (v/v)% ratios: [90-10], [80-20] and [70-30] where the first number corresponds to LCC30 volume content and the second to Al_2O_3.

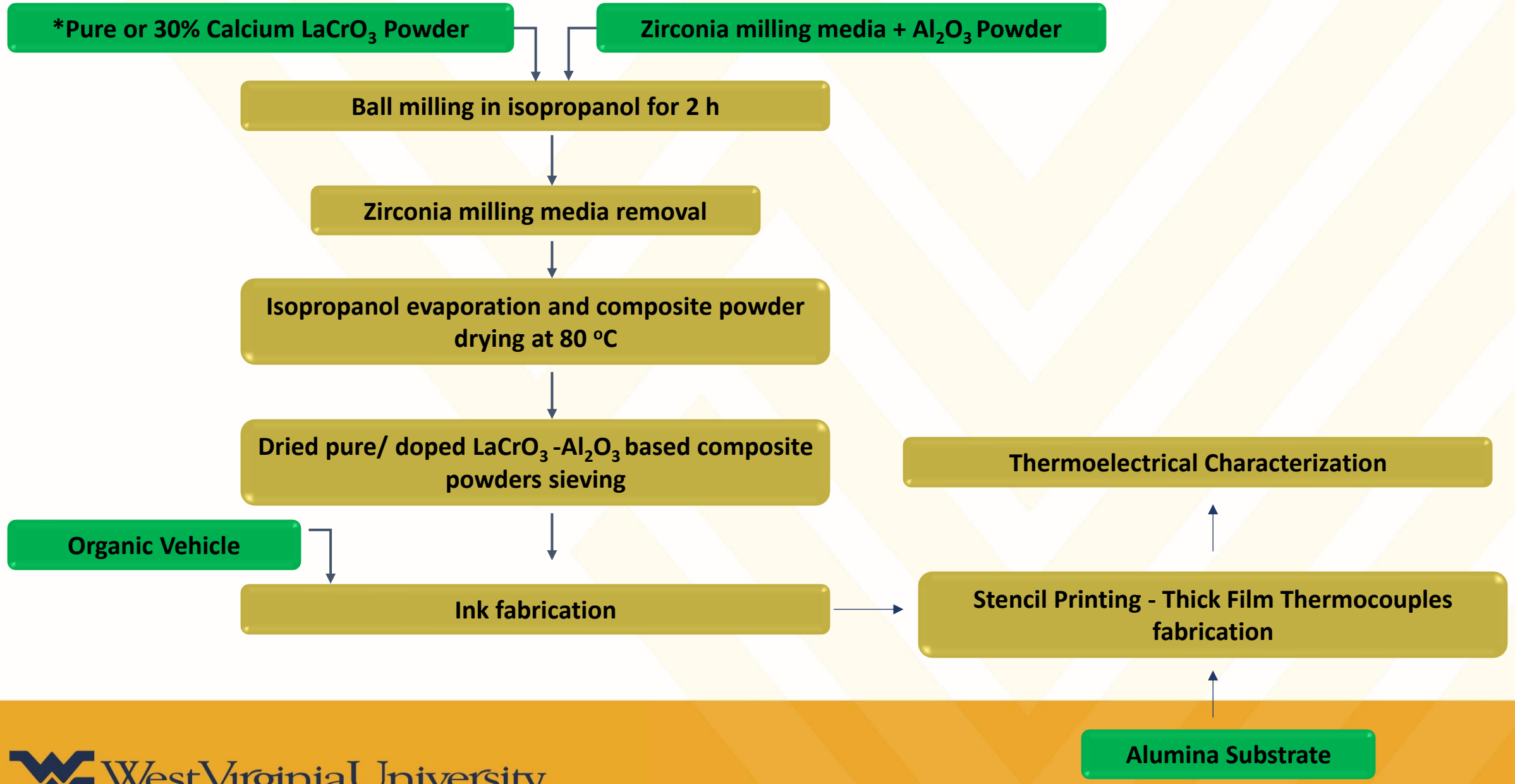
*Pure or 30% Calcium $LaCrO_3$ Powder
Zirconia milling media + Al_2O_3 Powder
Ball milling in isopropanol for 2 h
Zirconia milling media removal
Isopropanol evaporation and composite powder drying at 80 °C
Dried pure/ doped $LaCrO_3$ -Al_2O_3 based composite powders sieving
Organic Vehicle
Ink fabrication
Stencil Printing - Thick Film Thermocouples fabrication
Thermoelectrical Characterization
Alumina Substrate

Electrical Conductivity Characterization

DC Electrical Conductivity (Oxidizing Atmosphere)

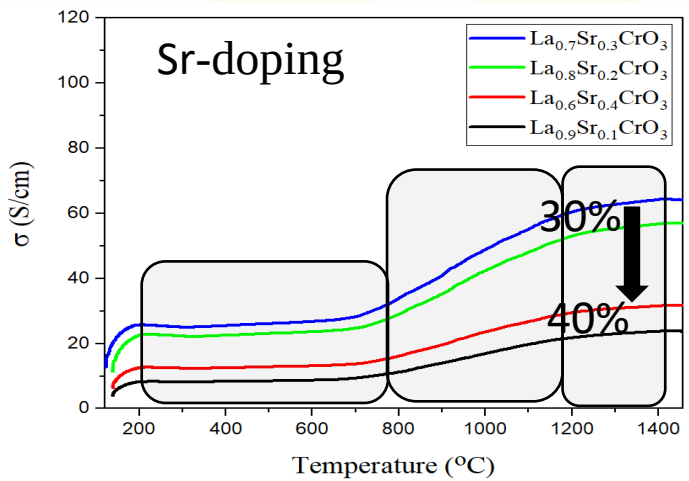

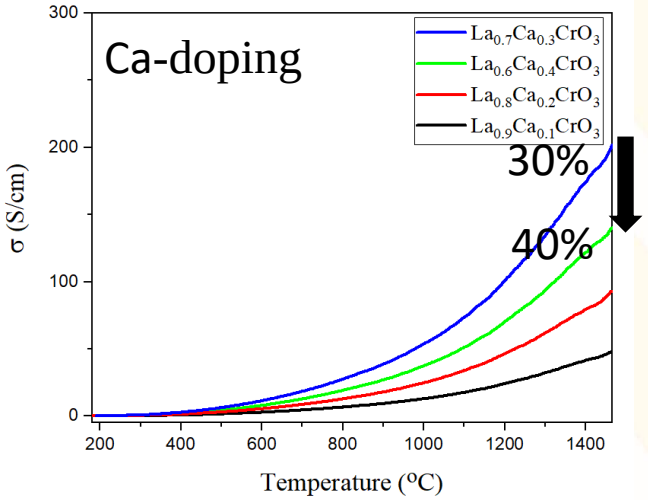

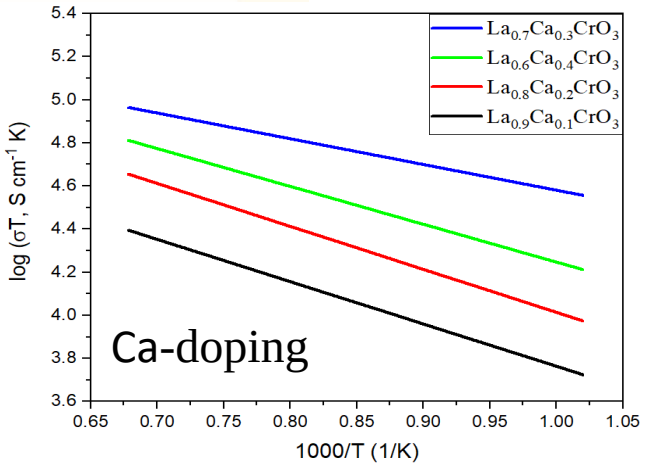

- Conductivity typically exponentially increases with increase in carrier mobility, but 30 to 40% all drop in conductivity (believe slight second phase or higher lattice strain).
- Sr doped shows three regions, not seen in literature, since most tests <850°-1000°C. (believe V_o at high temperature)
- Arrhenius relationship fits for higher temperature regimes.
- Calcium doped compositions present higher conductivity due the lower distortion effects on lattice structure.

Electrical conductivity vs temperature and Arrhenius Plot $La_{1-x}Sr_xCrO_3$, $La_{1-x}Ca_xCrO_3$

DC Electrical Conductivity (Reducing Atmosphere)

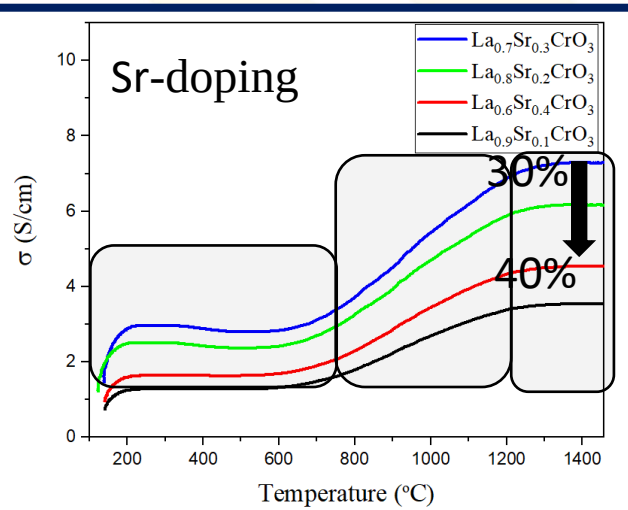

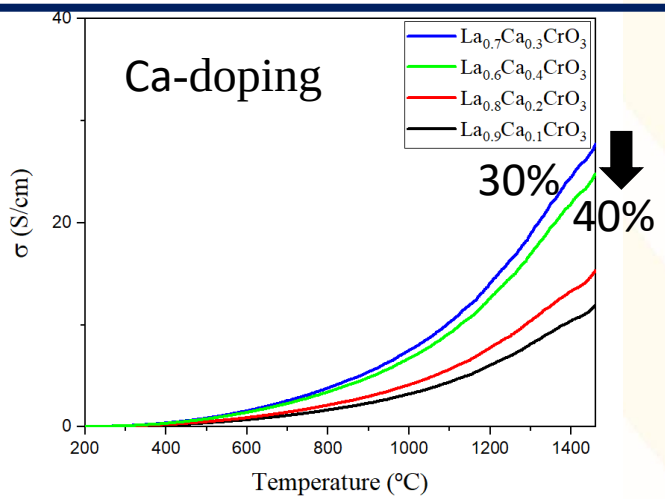

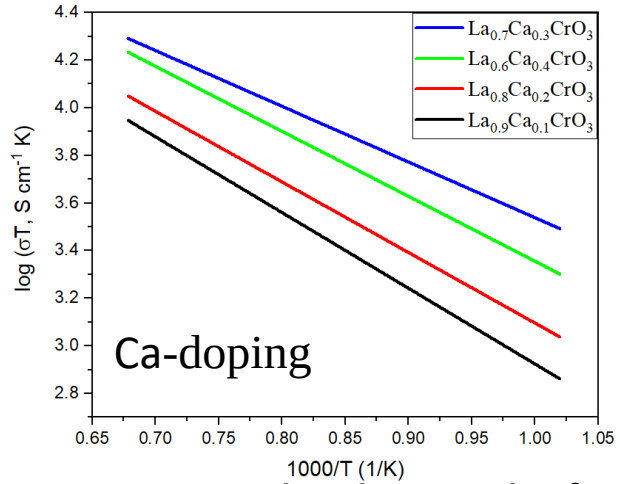

Electrical conductivity vs temperature and Arrhenius Plot for $La_{1-x}Sr_xCrO_3$, $La_{1-x}Ca_xCrO_3$

- Conductivity decrease for all temperature range under reducing atmosphere (H_2 5%/ N_2 95%).
- Under reducing conditions, oxygen vacancies form to keep neutrality (drop in hole carrier concentration).
- Sr conductivity still displays regions of altered mechanism.
- All compositions present lower conductivity as dopant increases (but still 40% lower than 30% in all cases).

Thick Film Sensors Fabrication

Thermoelectrical Characterization

High Temperature Sensors Fabrication

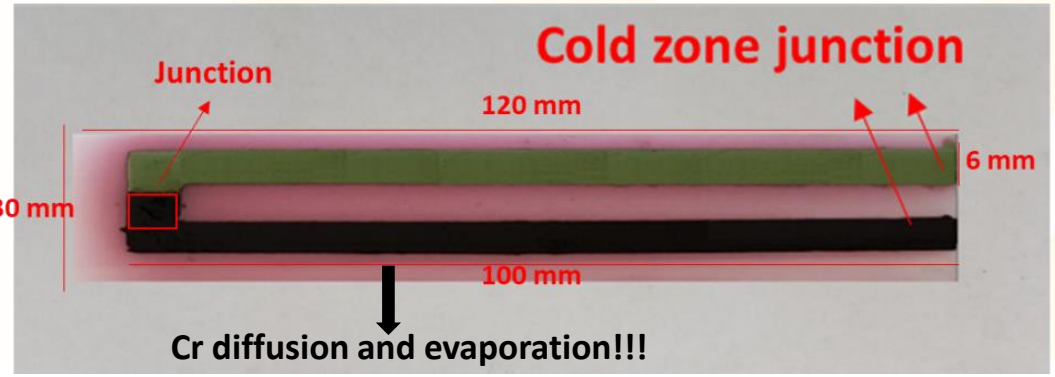

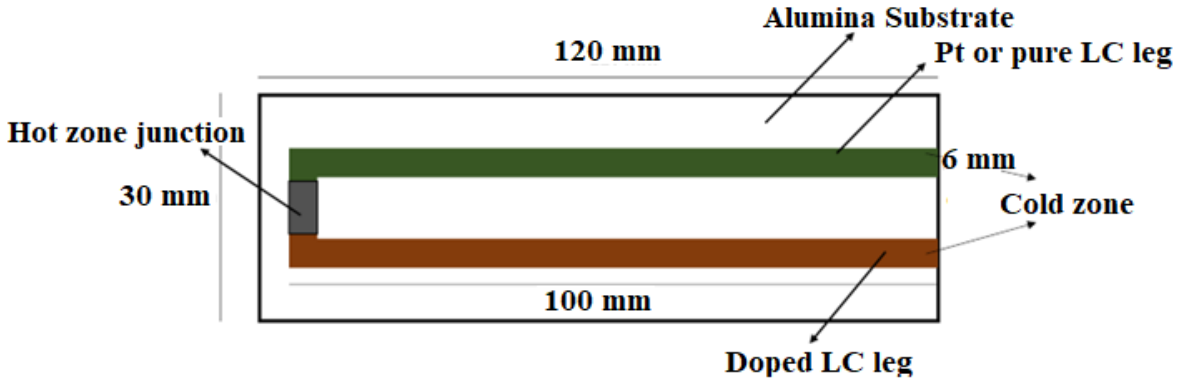

- Research team currently fabricating thermistors and thermocouples by 3D printing.
- High-temperature thermocouples that function >1200°C (in R-type range) new exciting development.

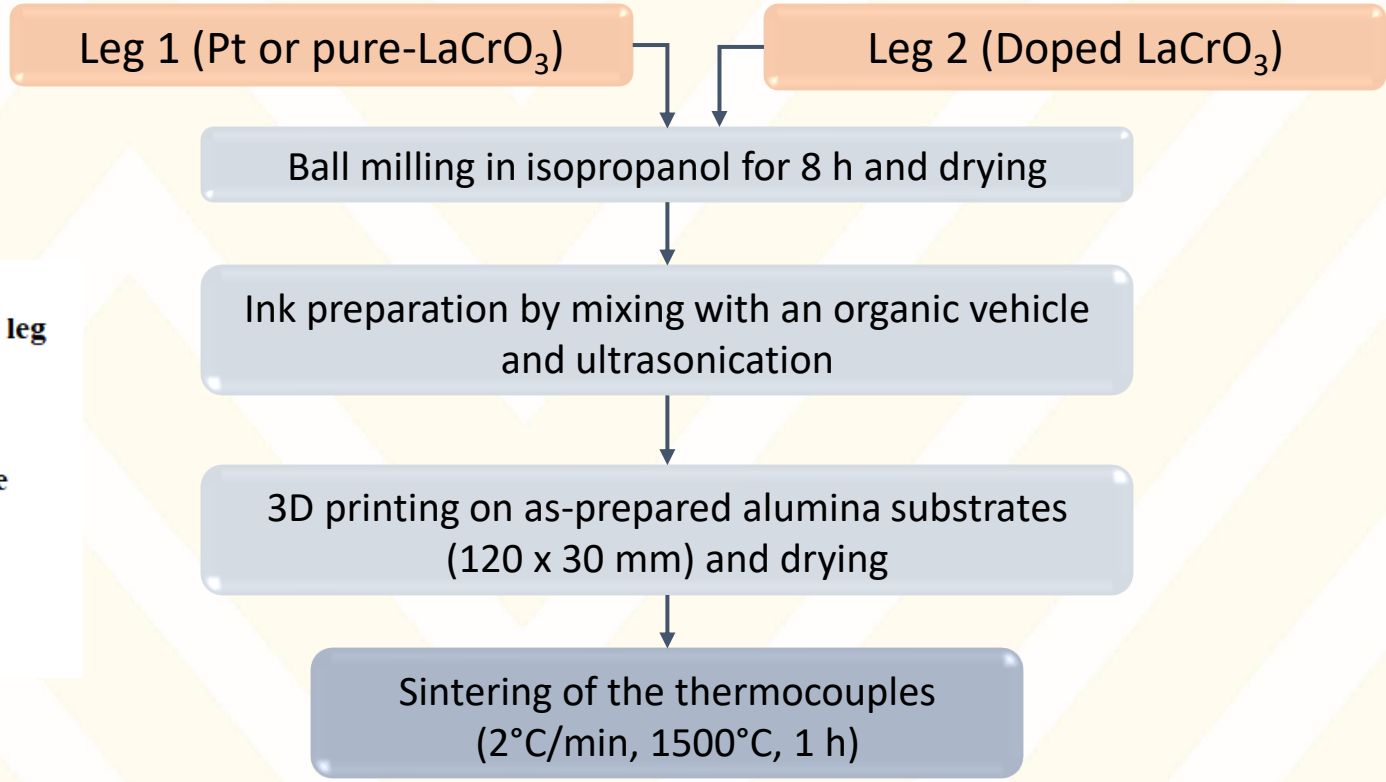

Seebeck Coefficient Estimation (Using Pt Standard)

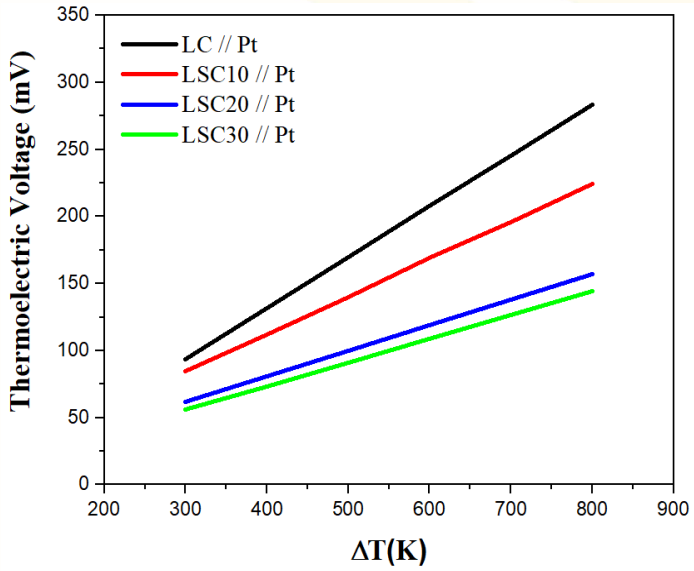

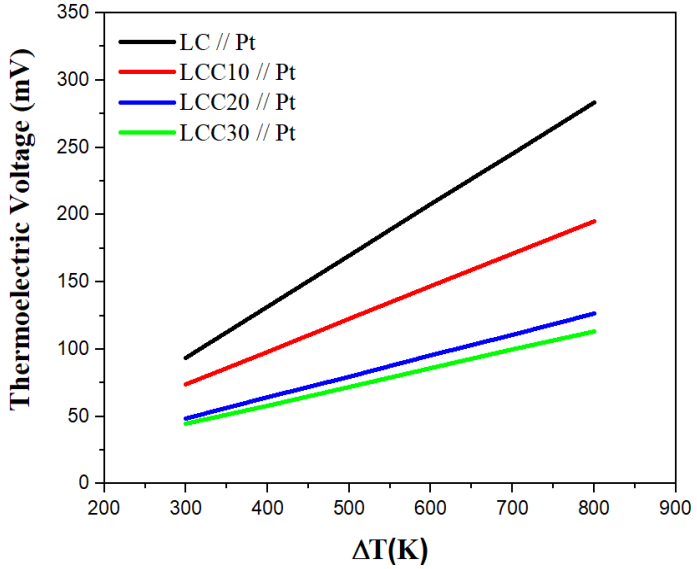

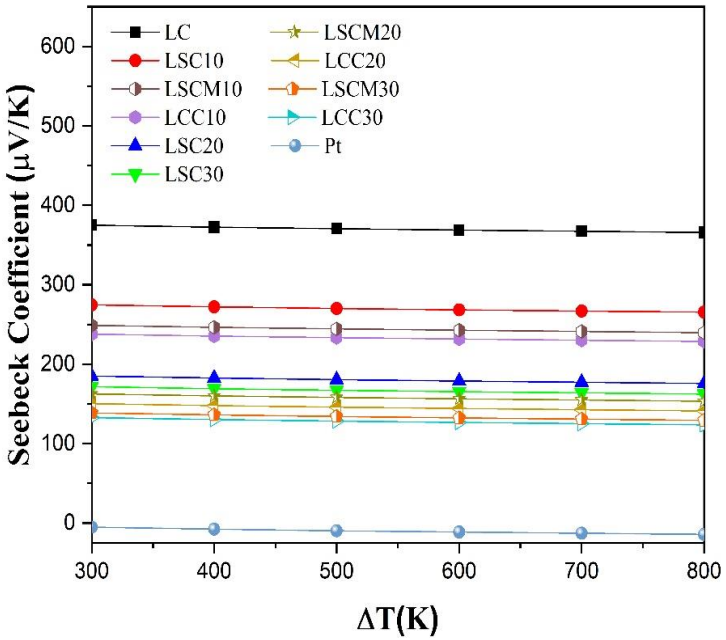

$$S(c) = (k_B/e)\ln[2(1-c)/c]$$

Heikes Equation

- Linear correlation between temperature difference and thermoelectric voltage was observed for all the compositions.
- Doped-$LaCrO_3$/Pt couples were fabricated to estimate intrinsic Seebeck coefficient (S_{Pt}~ -18 μV/K*) up to 1000°C.
- Ca doping shows lowest intrinsic Seebeck coefficient with increasing Ca content.

*Moore, J. P. (1973). *Journal of Applied Physics*. 44 (3): 1174–1178

Thermoelectric Characterization of Thermocouples

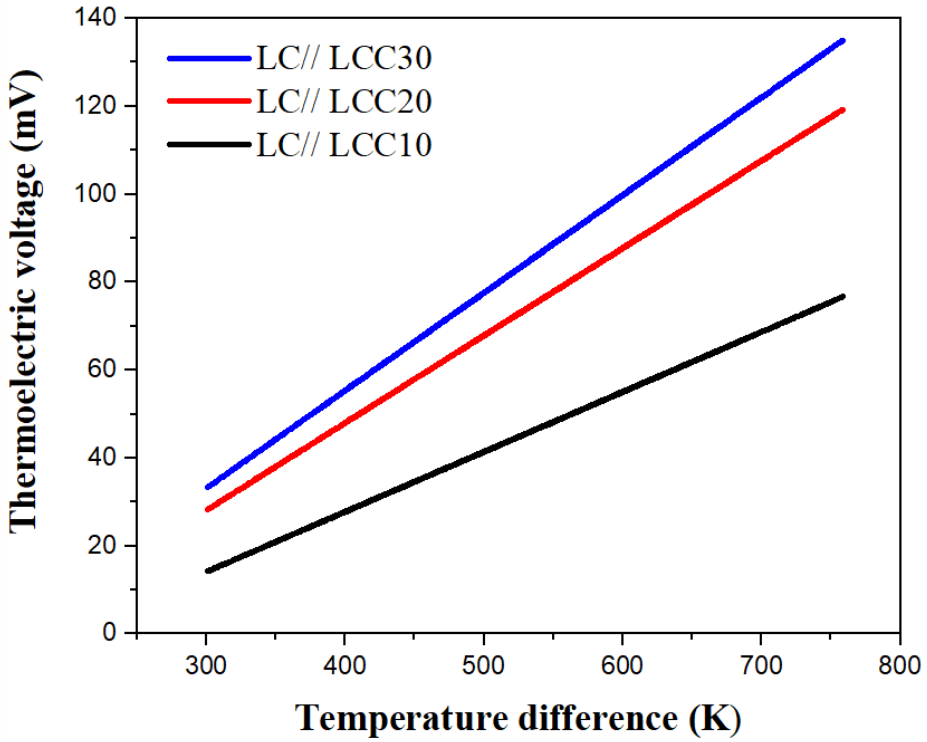

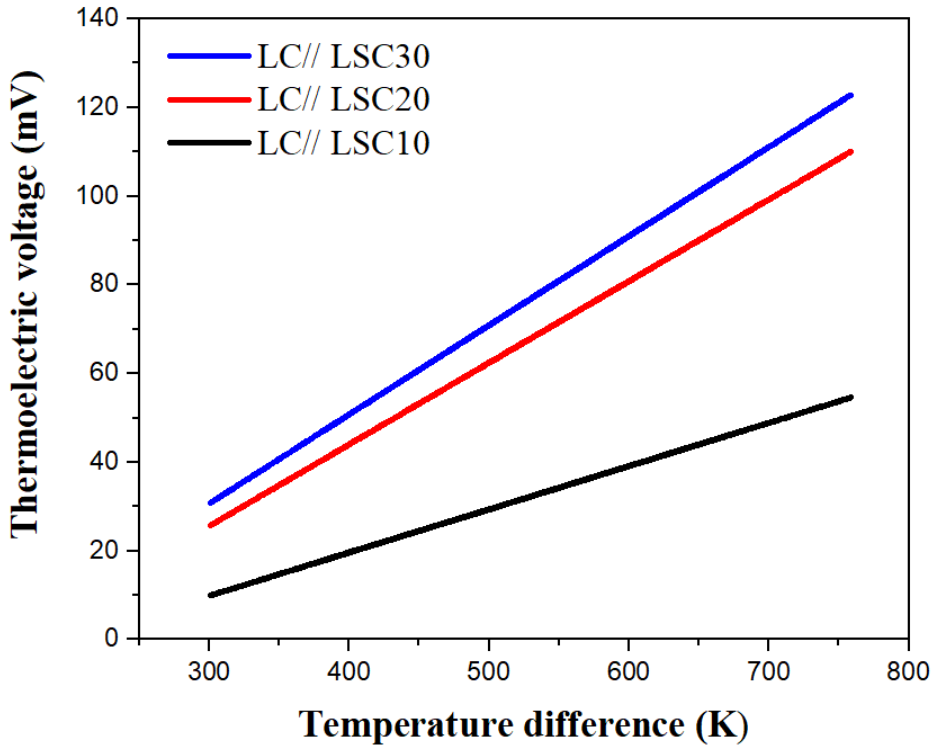

- Thermocouples were tested in a range between 30 to 850°C during 3 heating cycles, showing an excellent reproducibility.
- The LCC30/LC, LCC20/LC and LCC10/LC thermocouples showed a maximum higher voltage by **two orders of magnitude in comparison with Pt/Pt-Rh**, with values of 138.61 mV, 119.50 mV and 79.10 mV respectively (at ΔT~750°C).

Thermoelectric Characterization of Thermocouples

Thermoelectrical response of LCC30-Al_2O_3 composites // Pt

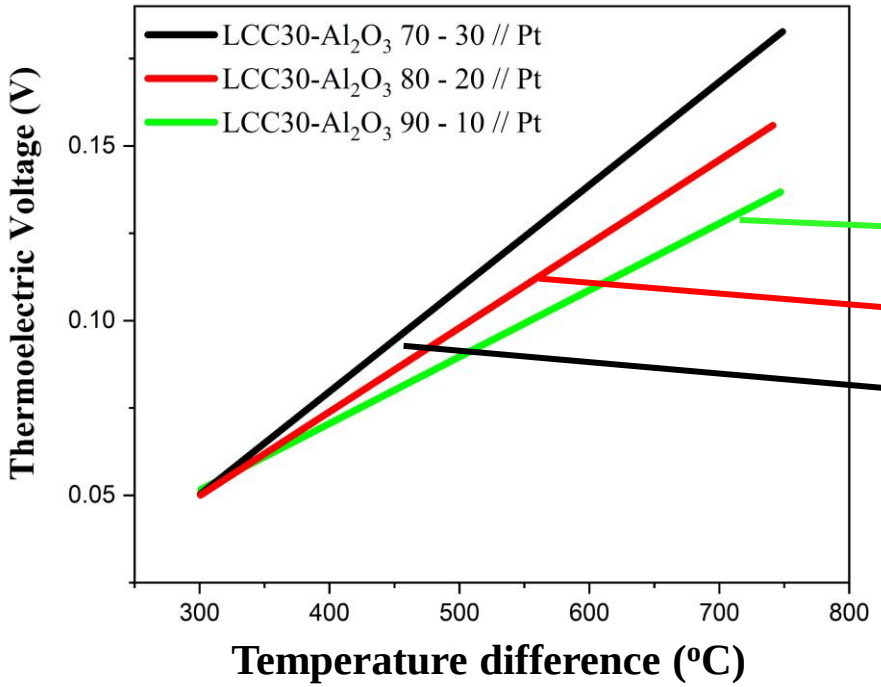

Electrical conductivity vs. temperature of LCC30-Al_2O_3 composites

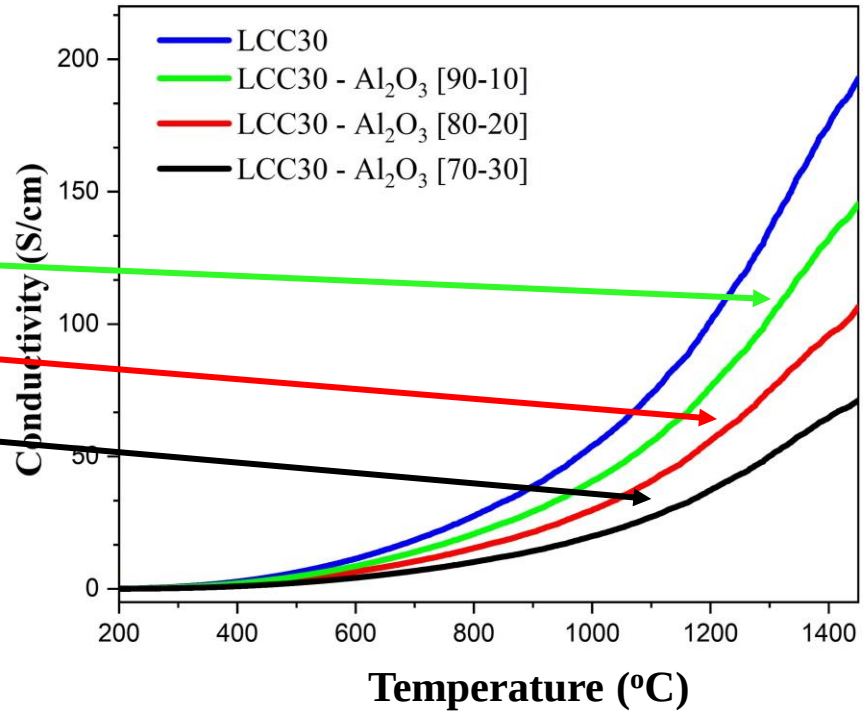

- Electrical conductivity and Thermoelectric voltage of LCC30-Al_2O_3 composites-based thick layer thermocouples were obtained.
- Inverse correlation between thermoelectric voltage response and electrical conductivity trends. Al_2O_3 content the resistivity of the composites and increase the thermoelectric output.

Thermoelectric Characterization of Thermocouples

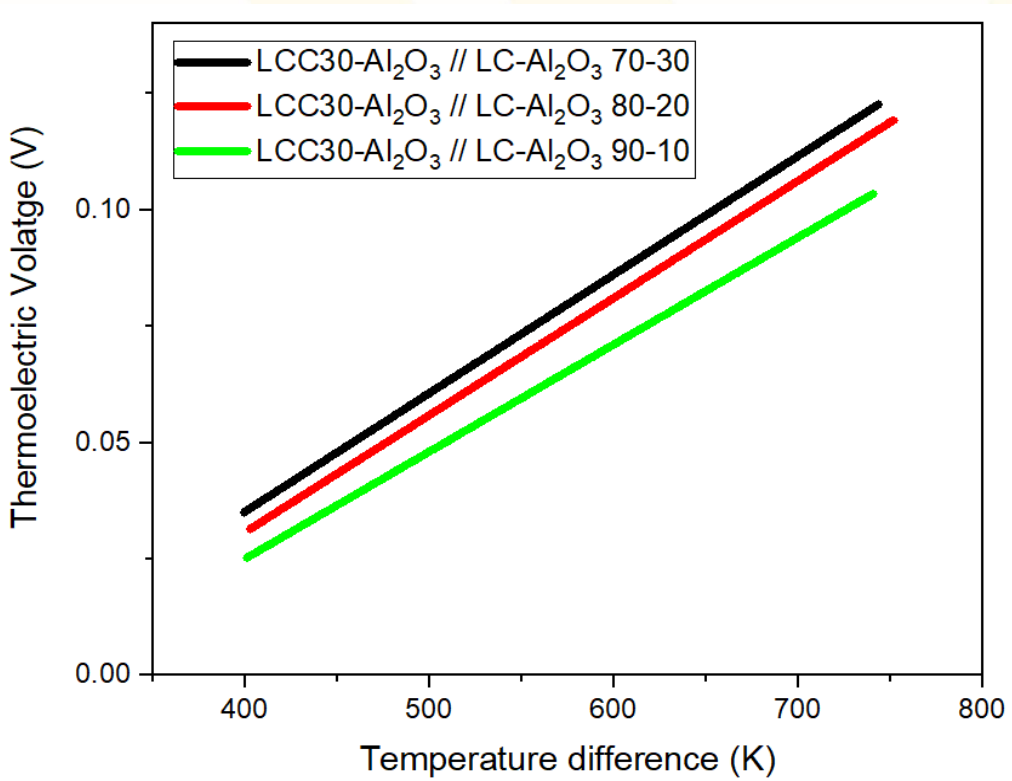

BSE - SEM

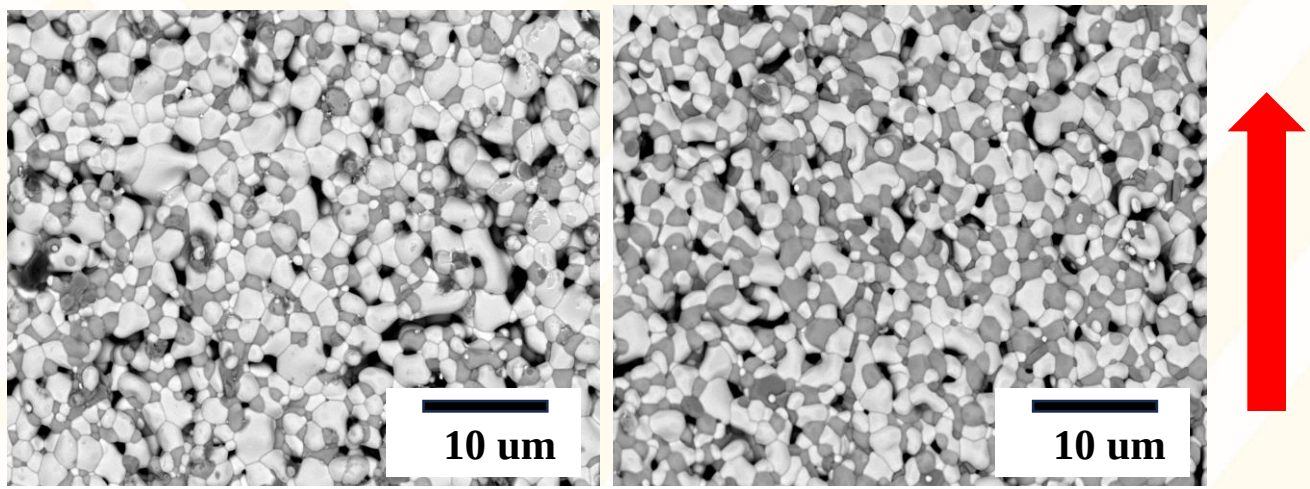

LCC30-Al_2O_3 [80-20] **LCC30-Al_2O_3 [70-30]**

Microstructures: LCC30 (white grains) - Al_2O_3/Aluminates (grey grains)

- LC-Al_2O_3 and LCC30-Al_2O_3 composites-based thick layer thermocouples fabricated were tested in a range between 30 to 850°C during showing linear correlation between thermoelectric voltage and temperature.
- Increase of Al_2O_3 content in thermocouples materials increase the driving potential by formation of aluminates secondary phases and higher concentration of Al_2O_3 grains.

Sensors Embedded into Refractory

Embedded Sensors Fabrication

General Smart Refractory Processing Method

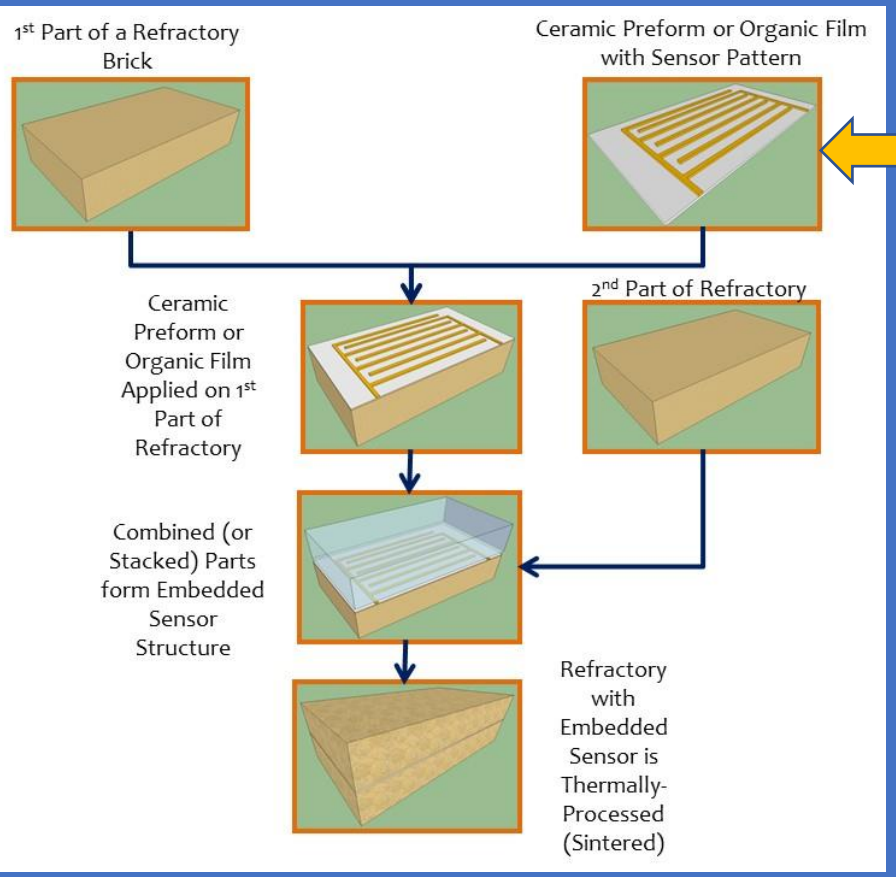

Examples of Sensor Preforms

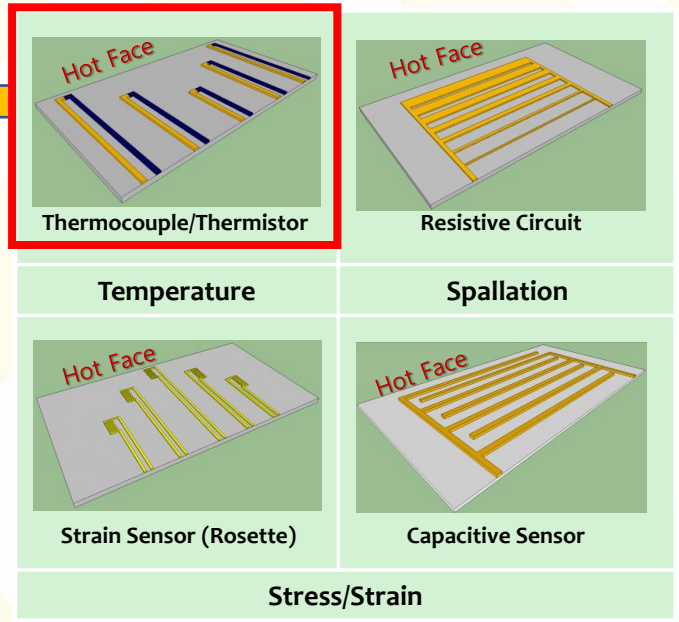

Embedded Thermocouples Characterization

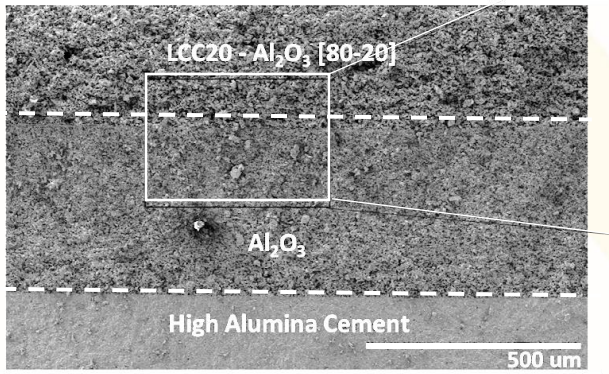

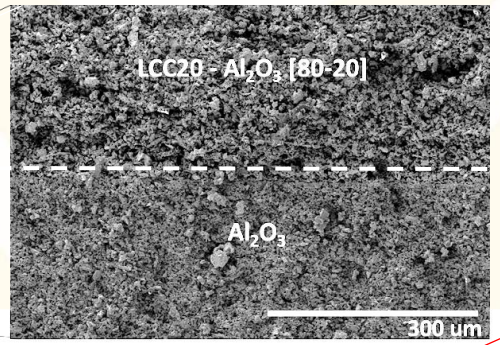

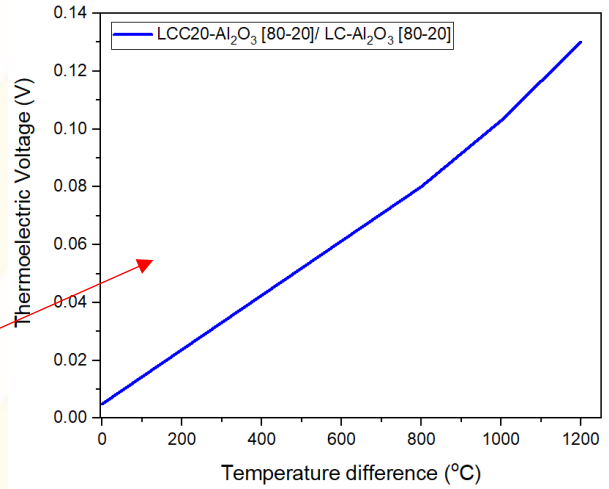

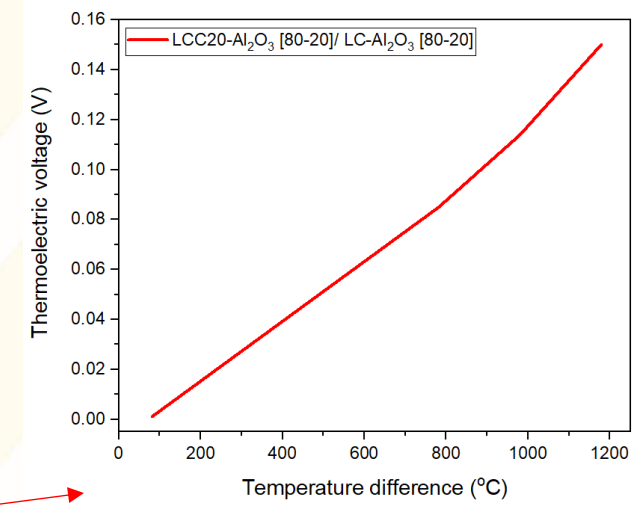

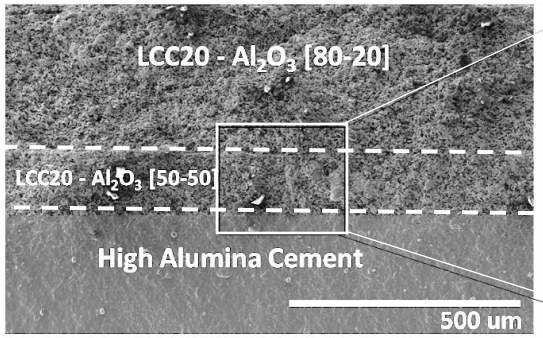

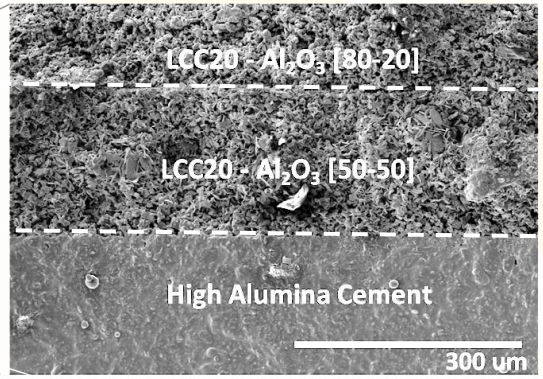

- Different 3D printing gradients were printed and embedded into high alumina refractory cement.
- Embedded thermocouples showed thermoelectric voltage responses ~ 0.15 V in at ΔT~1200°C

Conclusions

Conclusions

- Electrical conductivity shows correlated dependence with high temperature (up to 1500°C) for all compositions. The exponential Arrhenius trend is evidence for the polaron hopping electrical conduction mechanism.

- All the Seebeck coefficients were determined as the slope of the obtained plots, observing constant behavior as expected for polaron hopping active semiconductors such as doped $LaCrO_3$.

- It was observed that Seebeck coefficient reduces with the increase in dopant substituents as expected by Heikes model.

Conclusions

- **Embedded thermocouples into oxide refractories were fabricated using an easy approach.**
- **The embedded thermocouples showed a correlated increase in thermoelectric voltage (as expected) in function of temperature difference increment.**
- **Chromium diffusion was observed, there is a necessity for protect conductive layers and reduce chromium lost.**

Acknowledgment

❖We would like to thank U.S. Department of Energy (DOE) and Maria Reidpath (project manager) for sanctioning this project DE-FE0031825.

❖We also would like to acknowledge Mr. Harley Hart, Dr. Qiang Wang, and Dr. Marcela Redigolo for their cooperation and valuable assistance in the WVU Shared Research Facilities (SRF).

❖We also would like to thank HWI, for support us in developing real-life applications sensing systems/devices.

❖Kindly acknowledge faculty and staff of West Virginia University for their support.

Thank you for the attention.

Email: jam00009@mix.wvu.edu

Email: Ed.Sabolsky@mail.wvu.edu

Electrical Conductivity (Oxygen partial pressure)

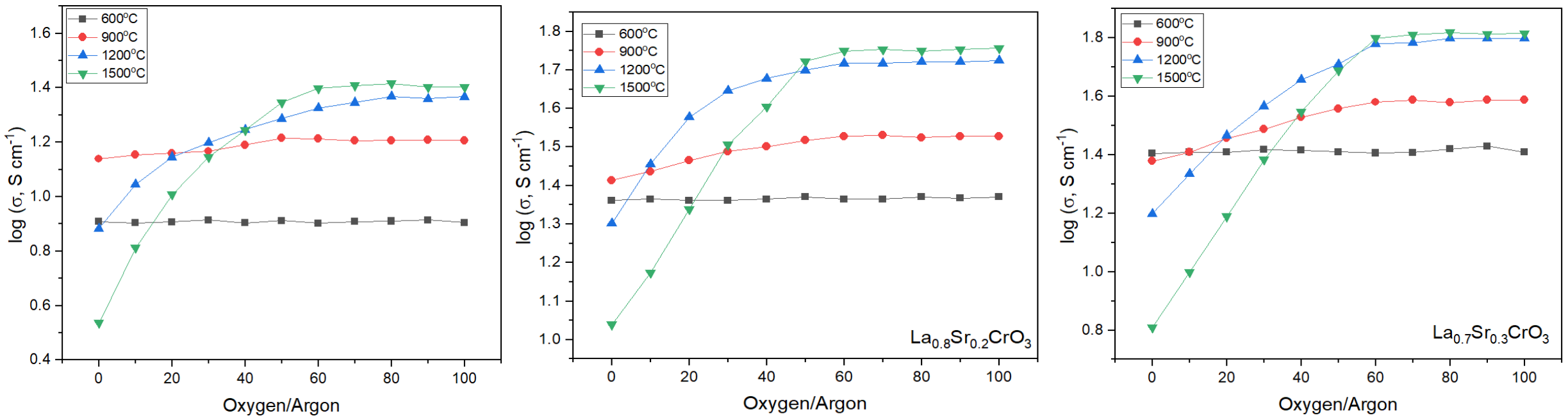

Electrical conductivity dependence of oxygen partial pressures at different temperatures for $La_{1-x}Sr_xCrO_3$

- At lower temperatures (600°C - 900°C) not significant changes in conductivity occurs for lanthanum doped compositions during the equilibrium time used (90 minutes).
- At higher temperatures (1200°C and 1500°C) the conductivity drops exponentially at lower oxygen partial pressures. Increasing the strontium concentration, the conductivity drop significantly.

Electrical Conductivity (Oxygen partial pressure)

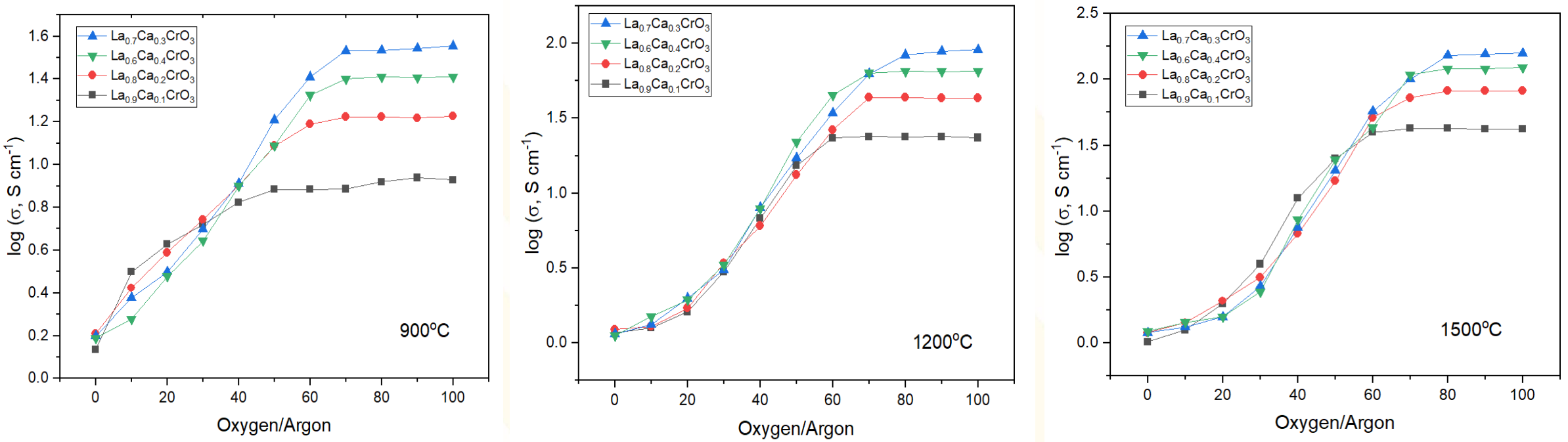

Electrical conductivity dependence of oxygen partial pressures at different temperatures for $La_{1-x}Ca_xCrO_3$

- When the oxygen partial pressure goes below a critical value, the oxygen vacancies are generated at expense of electron holes and conductivity decrease for all compositions.
- The charge imbalance caused by the introduction of Calcium starts to be compensated by the formation of oxygen vacancies.

Sr doped lanthanum chromite stability experiments

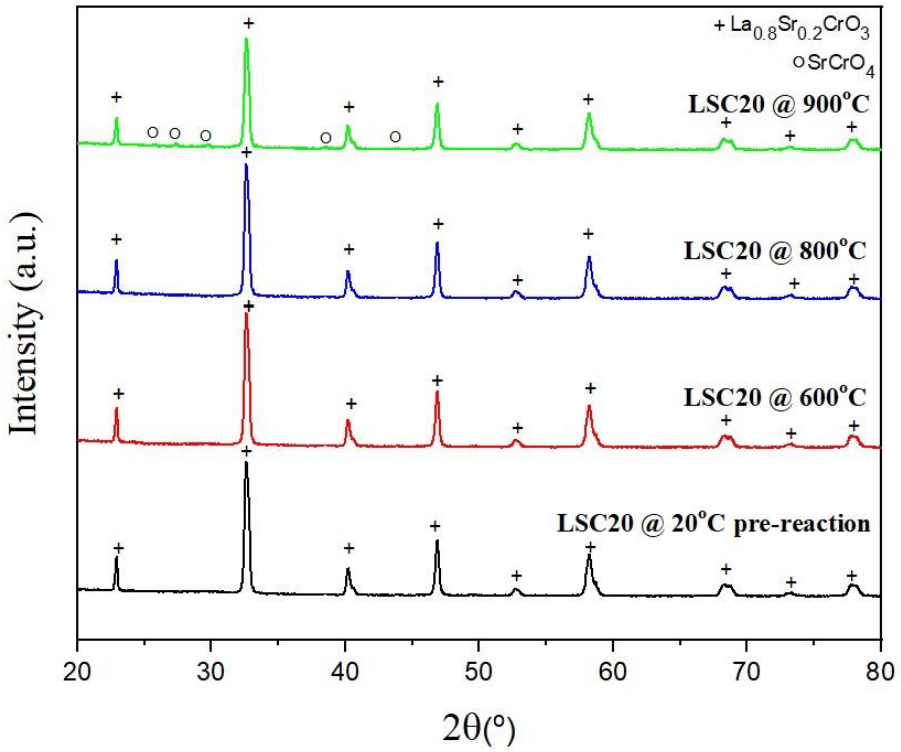

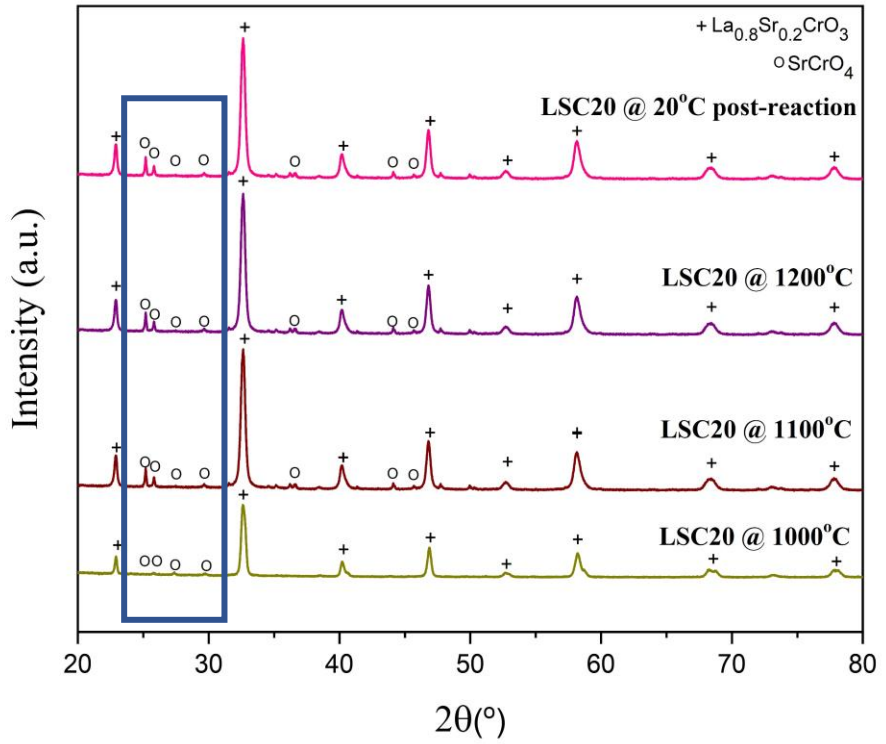

X-ray diffractograms of 20% strontium doped lanthanum chromite annealed at different temperatures.

Crystalline Structure/Phase Analysis

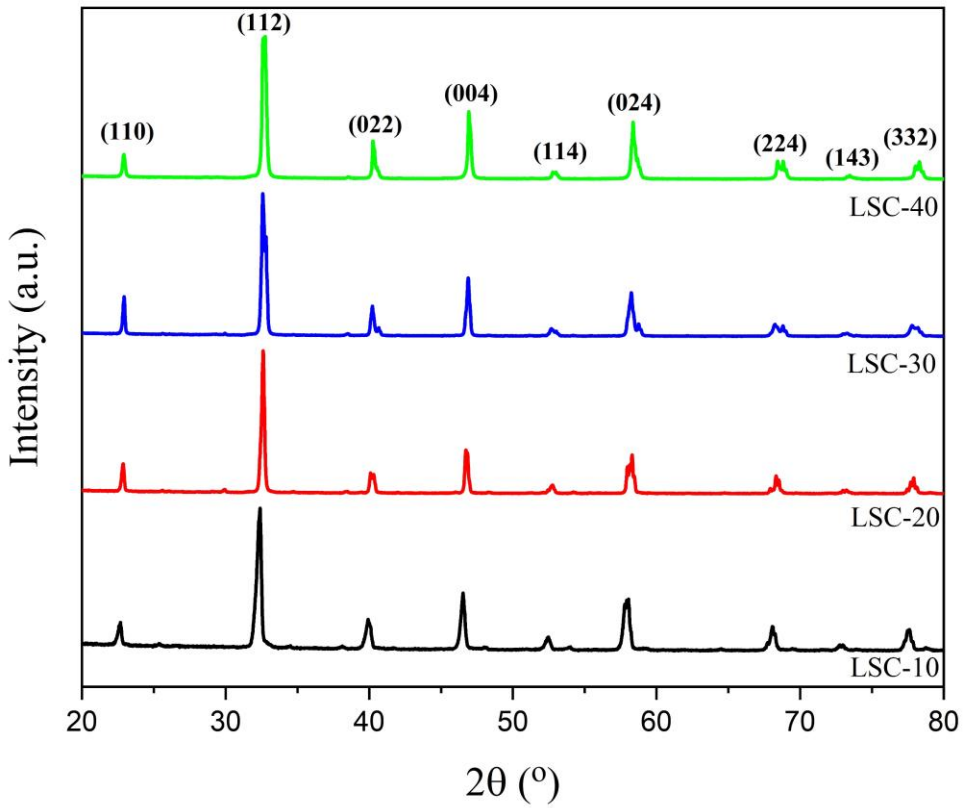

X-ray diffractograms for the samples of the $La_{1-x}Sr_xCrO_3$ series

- Single phase doped lanthanum chromites materials were obtained successful (no residual oxide or pyrochlore peaks).
- Using Pechini Sol-Gel method permitted doped lanthanum chromites at high solubility levels (40%).
- Solubility limits >40% substitution level (Sujatha *et al.* 1992).
- No impurities extra peaks were present in the final prepared powders and ceramic pellets.

Lattice Parameters, Unit Cell Volume and Density

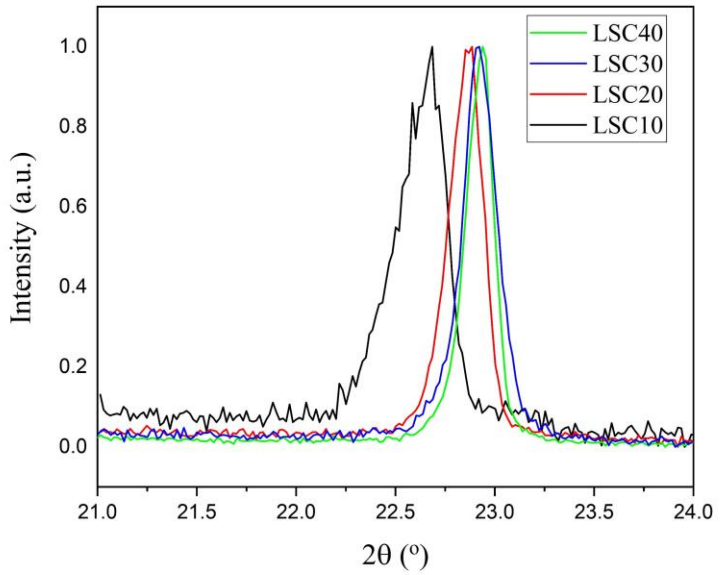

X-ray diffractograms showing shifting of (110) peak for the $La_{1-x}Sr_xCrO_3$ series

Lattice parameters, unit cell volume and XRD theoretical density for doped lanthanum chromites perovskites

Composition	Lattice parameters (Å)			Volume ($Å^3$)	$\rho XRD_{Theoretical}$ (g/cm^3)
	a	b	c		
$La_{0.9}Sr_{0.1}CrO_3$	5.5124	5.5668	7.7926	239.1299	6.4932
$La_{0.8}Sr_{0.2}CrO_3$	5.4988	5.5425	7.7853	237.2747	6.4004
$La_{0.7}Sr_{0.3}CrO_3$	5.4769	5.5233	7.7580	234.6839	6.3259
$La_{0.6}Sr_{0.4}CrO_3$	5.4524	5.5122	7.7407	232.6441	6.2350
$La_{0.9}Ca_{0.1}CrO_3$	5.4180	5.5039	7.7332	230.6050	6.5963
$La_{0.8}Ca_{0.2}CrO_3$	5.4092	5.4982	7.7264	229.7898	6.3341
$La_{0.7}Ca_{0.3}CrO_3$	5.3994	5.4877	7.7058	228.3264	6.0872
$La_{0.6}Ca_{0.4}CrO_3$	5.3897	5.4622	7.6853	226.2520	5.8528
$La_{0.8}Sr_{0.20}Cr_{0.90}Mn_{0.10}O_3$	5.4734	5.5648	7.7765	236.8595	6.1533
$La_{0.8}Sr_{0.20}Cr_{0.80}Mn_{0.20}O_3$	5.4705	5.5587	7.7702	236.2829	6.1766
$La_{0.8}Sr_{0.20}Cr_{0.70}Mn_{0.30}O_3$	5.4598	5.5398	7.7498	234.4020	6.2344
$La_{0.8}Sr_{0.20}Cr_{0.60}Mn_{0.40}O_3$	5.4146	5.4981	7.7065	229.4225	6.3783

%Sr↑

%Ca↑

%Mn↑

- Decrease in lattice parameters (and volume) were observed when dopant cations is introduced in the lattice.
- To achieve neutrality chromium change from Cr^{+3} to Cr^{+4}, reduction in the chromium size occurs (Hyun Choi *et al.* 2013) .

Microstructure/Grain Size Distribution

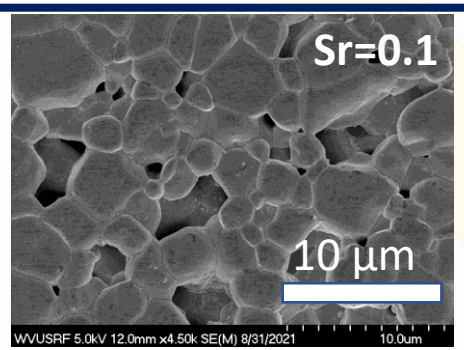

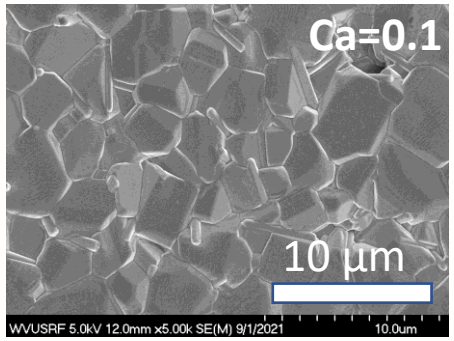

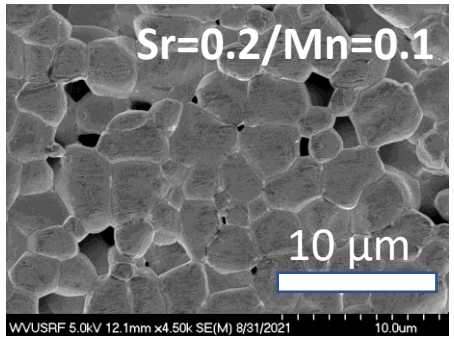

Average grain size and bulk density distribution for $La_{1-x}Sr_xCrO_3$, $La_{1-x}Ca_xCrO_3$ series

Composition	Average Grain Size (µm)	Relative Percentage Bulk Density (%)	
$La_{0.9}Sr_{0.1}CrO_3$	3.6	94	%Sr↑
$La_{0.8}Sr_{0.2}CrO_3$	3.5	95	
$La_{0.7}Sr_{0.3}CrO_3$	3.6	95	
$La_{0.6}Sr_{0.4}CrO_3$	3.2	94	
$La_{0.9}Ca_{0.1}CrO_3$	4.1	96	%Ca↑
$La_{0.8}Ca_{0.2}CrO_3$	3.7	97	
$La_{0.7}Ca_{0.3}CrO_3$	3.7	97	
$La_{0.6}Ca_{0.4}CrO_3$	3.6	98	

- Pechini Sol Gel prepared calcium, strontium, manganese doped lanthanum chromite powders exhibit better sinterability and densification under oxidizing conditions (undoped ↓90%).
- The samples of Ca doped lanthanum chromite powder have more dense microstructures. Furthermore, it was found that the incorporation of Ca, Sr in the A site of the lanthanum chromite increases grain growth (undoped <3 µm).

DC Electrical Conductivities/Activation Energies

Composition	Air Atmosphere		Reducing Atmosphere	
	Conductivity @ 1000°C (S/cm)	Activation energy (eV)	Conductivity @ 1000°C (S/cm)	Activation energy (eV)
$La_{0.9}Sr_{0.1}CrO_3$	16.672	0.1552	2.691	0.3238
$La_{0.8}Sr_{0.2}CrO_3$	42.882	0.1427	4.572	0.2597
$La_{0.7}Sr_{0.3}CrO_3$	49.032	0.1055	5.534	0.1719
$La_{0.6}Sr_{0.4}CrO_3$	23.599	0.1498	3.462	0.3102
$La_{0.9}Ca_{0.1}CrO_3$	13.211	0.1417	3.152	0.3240
$La_{0.8}Ca_{0.2}CrO_3$	24.170	0.1298	4.118	0.2103
$La_{0.7}Ca_{0.3}CrO_3$	52.823	0.1028	7.602	0.1367
$La_{0.6}Ca_{0.4}CrO_3$	38.152	0.1175	6.626	0.1747

$$\sigma = \frac{\sigma_0}{T}\exp\left(\frac{-\Delta E_a}{kT}\right)$$

Slope $\propto E_a$

- Conductivity increase as function of doping level up to 30% for all dopants (strontium, calcium and manganese).
- At 40% doping levels conductivity decrease due to higher lattice distortion in all systems (solubility limit).
- Lower conductivity values under reducing atmospheres are explained by oxygen vacancies formation (near >1.5× in activation energy).

Ca doped lanthanum chromite stability experiments

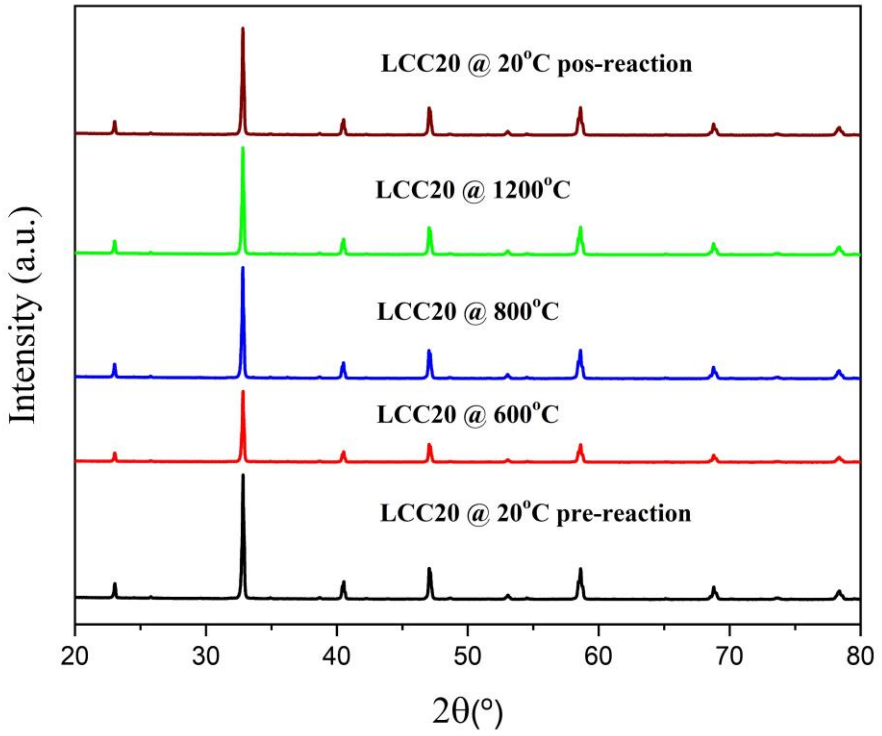

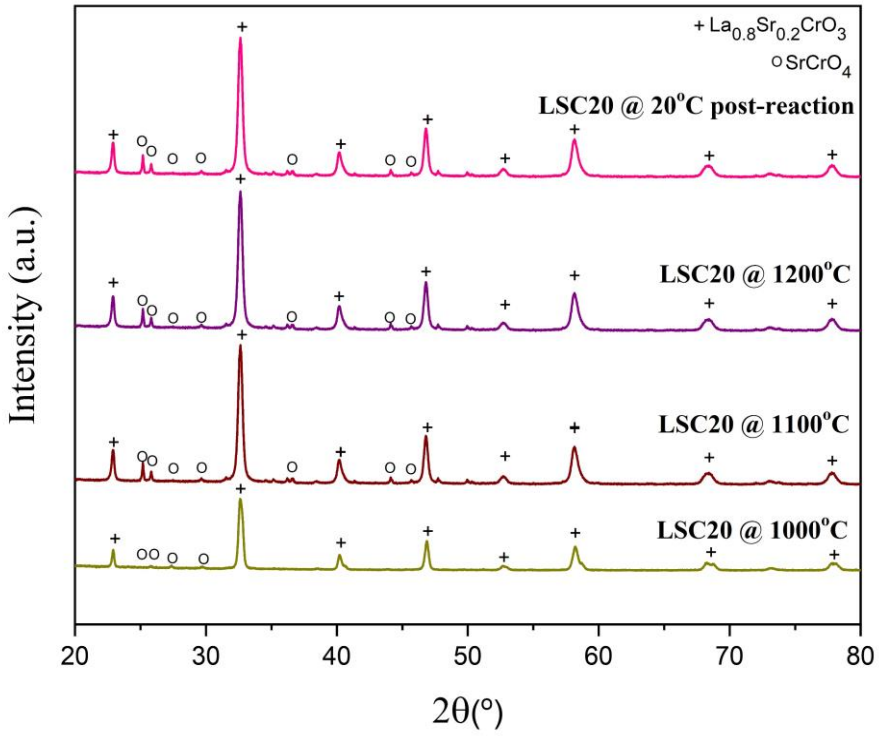

X-ray diffractograms of 20% strontium and calcium doped lanthanum chromite annealed at different temperatures.

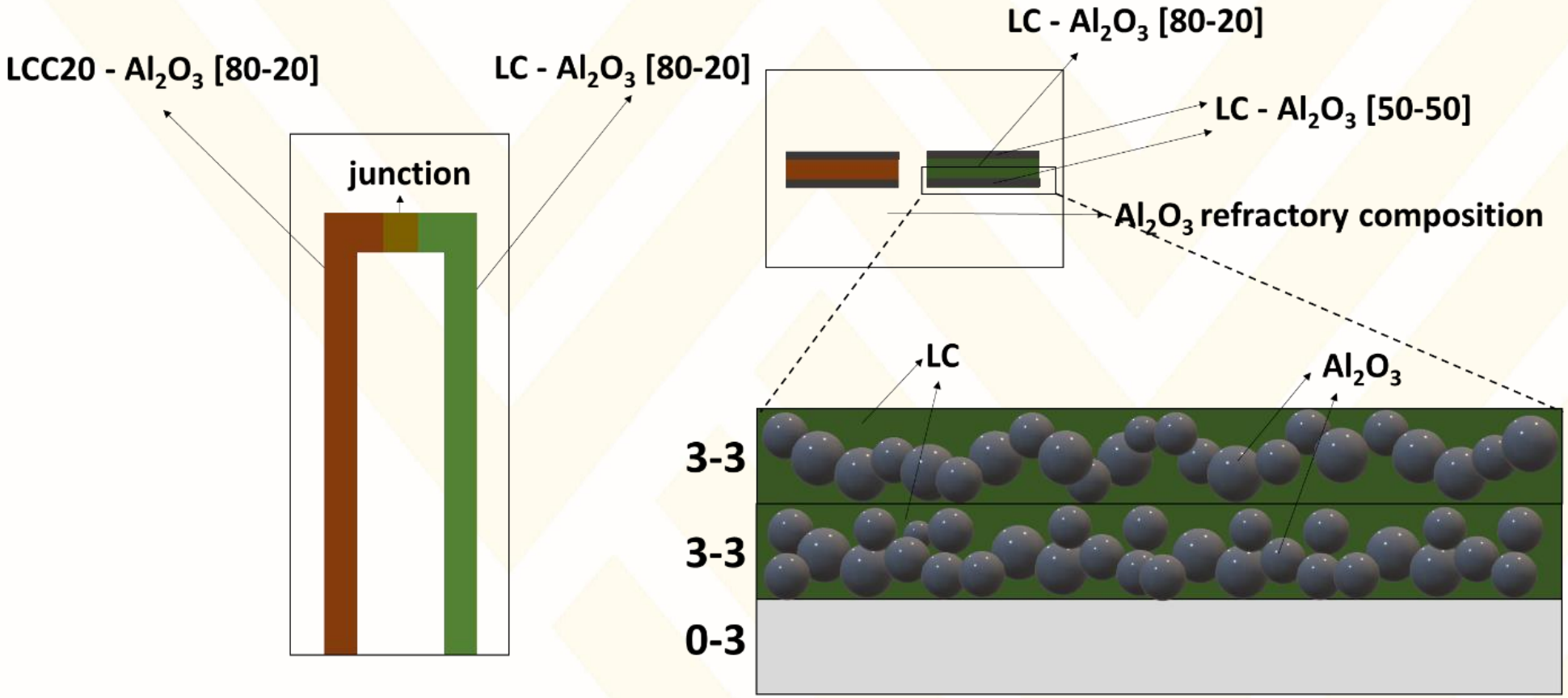
LCC20 - Al_2O_3 [80-20]
LC - Al_2O_3 [80-20]
junction
LC - Al_2O_3 [80-20]
LC - Al_2O_3 [50-50]
Al_2O_3 refractory composition
LC
Al_2O_3
3-3
3-3
0-3

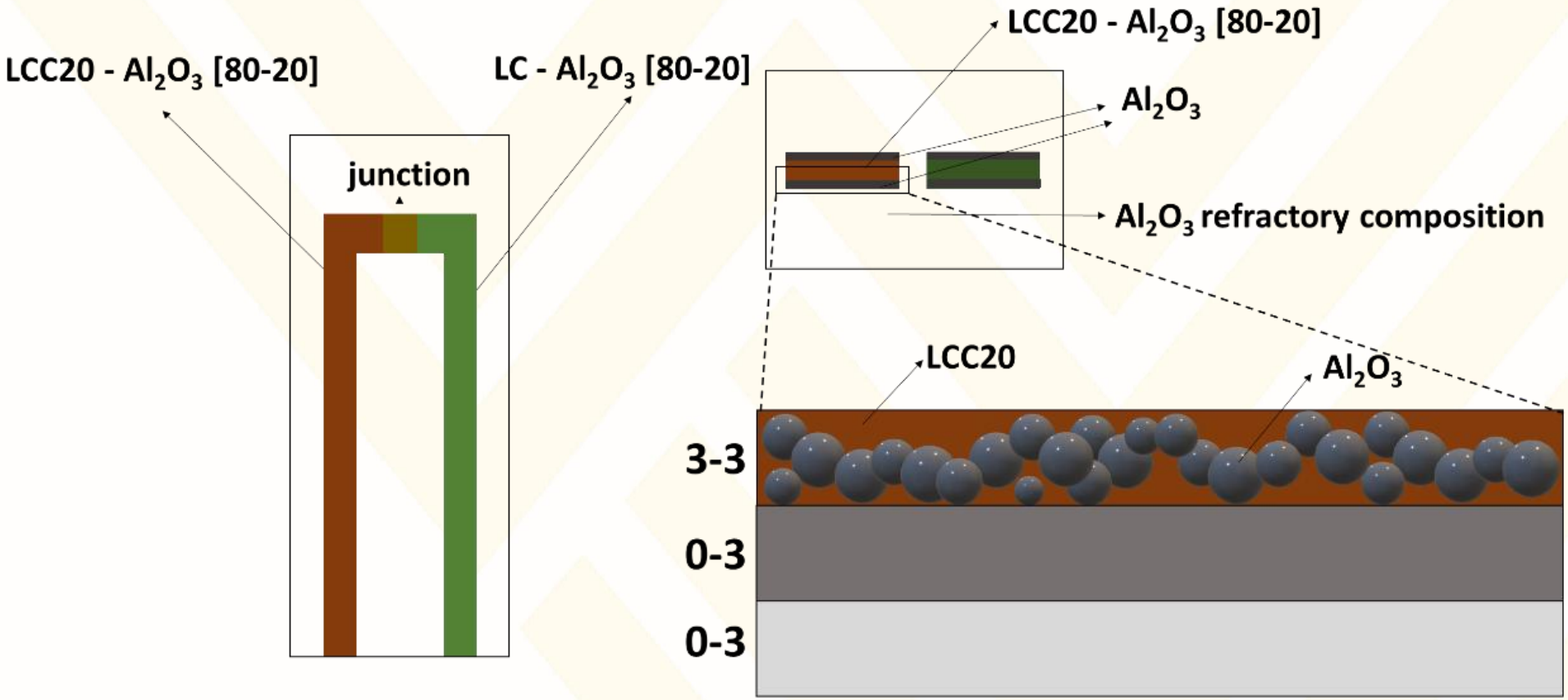
LCC20 - Al_2O_3 [80-20]
LC - Al_2O_3 [80-20]
junction
LCC20 - Al_2O_3 [80-20]
Al_2O_3
Al_2O_3 refractory composition
LCC20
Al_2O_3
3-3
0-3
0-3

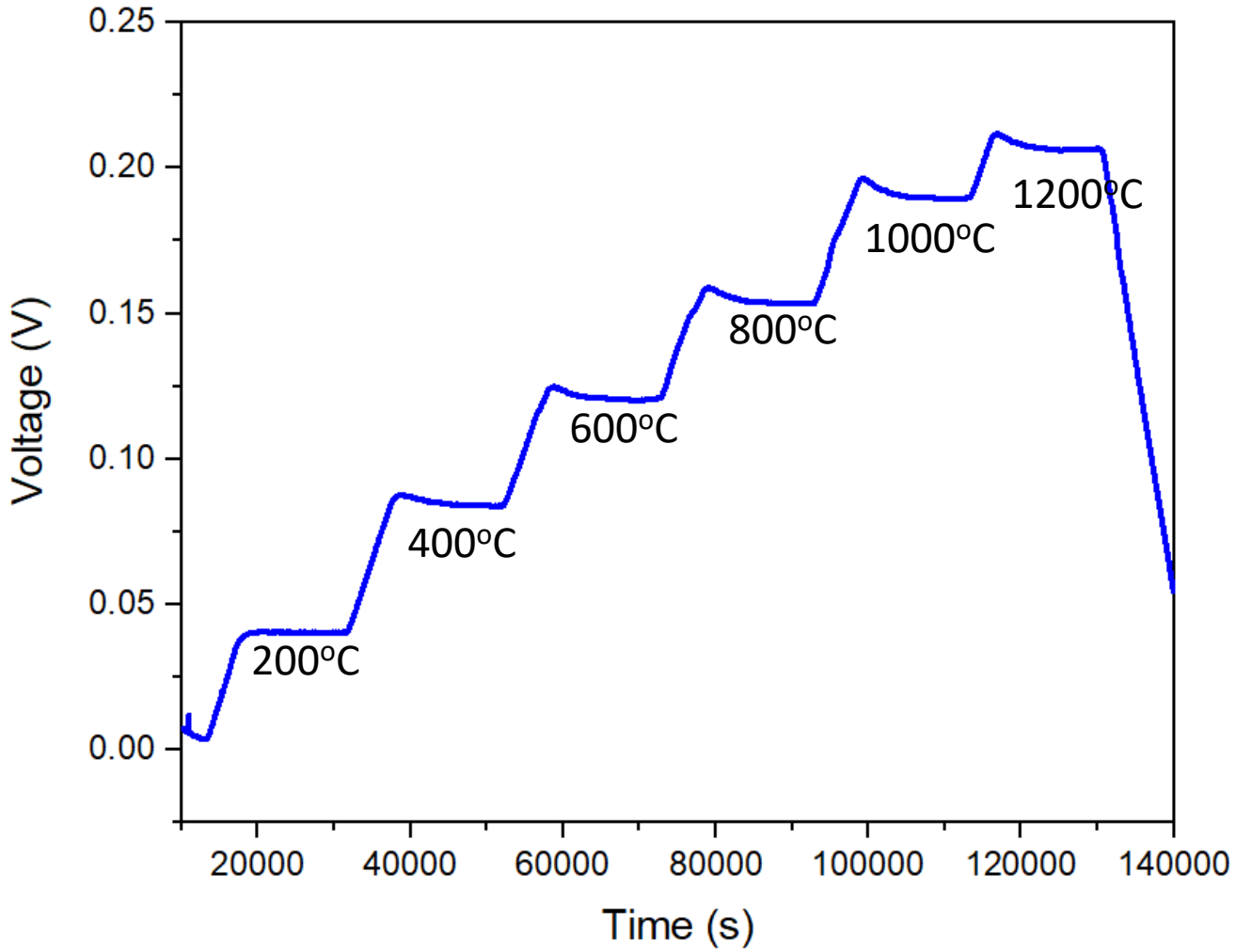

1 Alumina layer
1 LCC/ Alumina 95/5 layer
1 Alumina layer

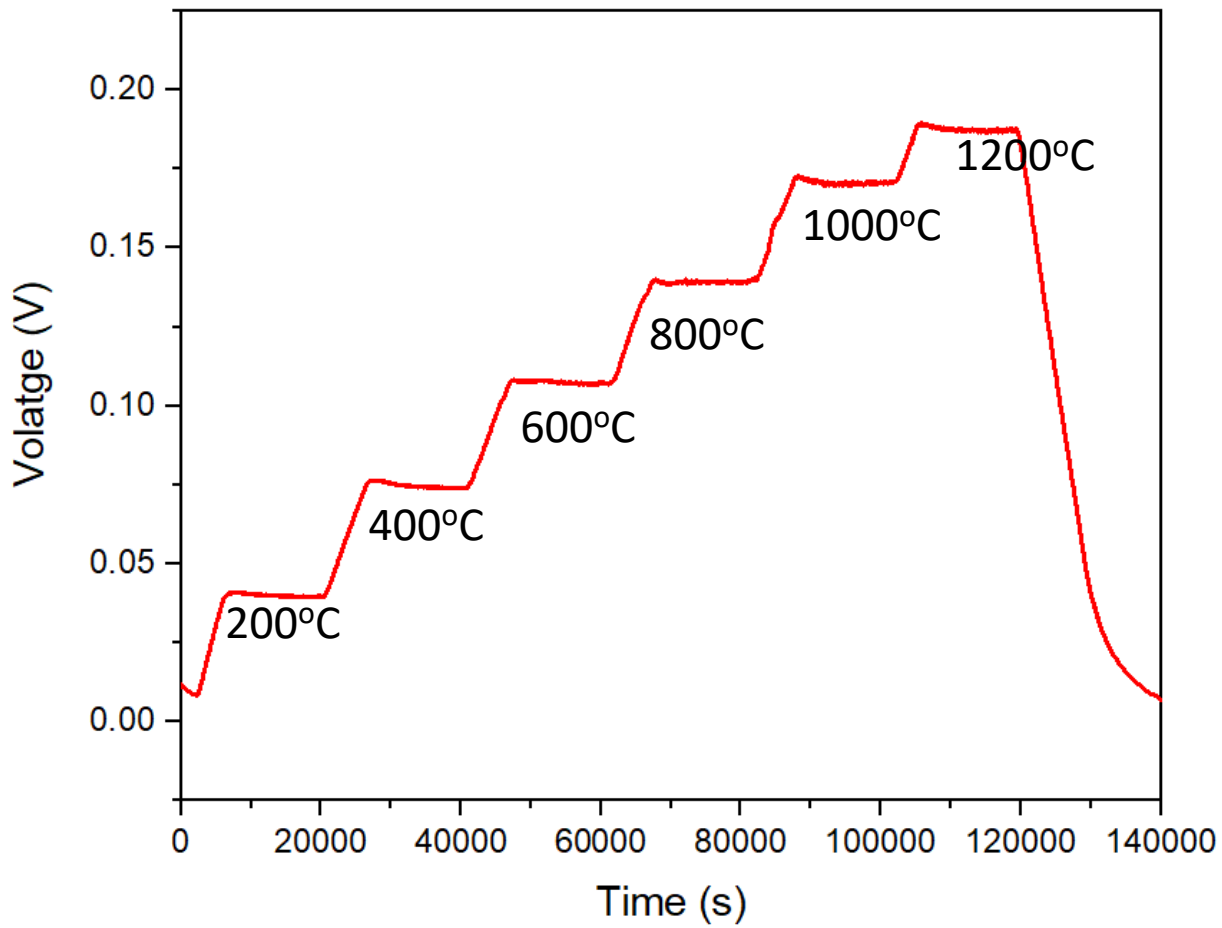

2 layers LCC20
2 Layers LC

XRD - Composites characterization

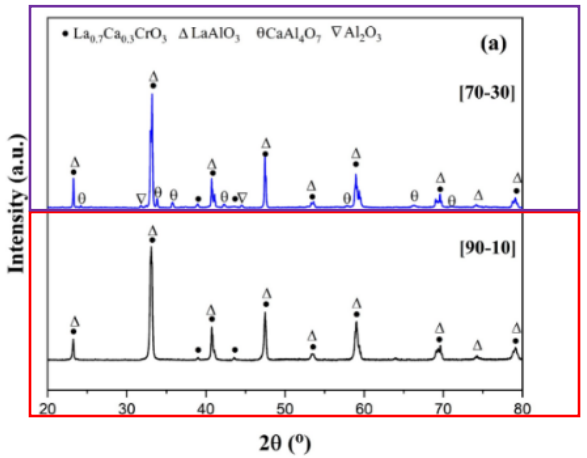

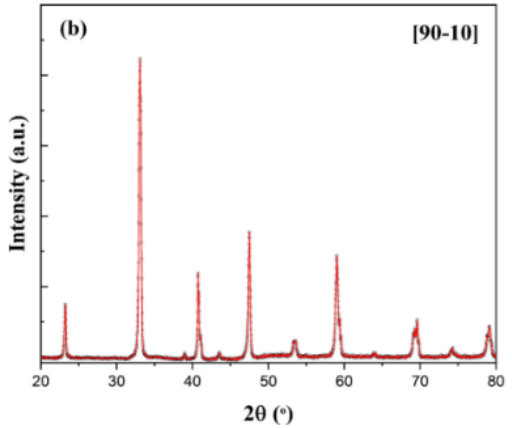

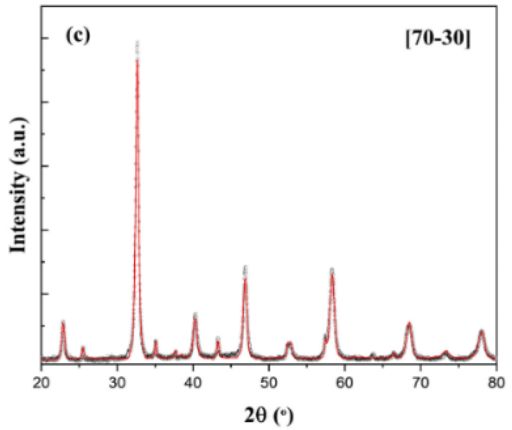

- LCC30-Al_2O_3 [90-10] indicates that LCC30 phase was present, and a secondary lanthanum aluminate was formed during the sintering process.
- LCC30-Al_2O_3 [70-30] diffractogram shows LCC30 and lanthanum aluminate ($LaAlO_3$), calcium aluminate ($Ca_2Al_2O_5$) and pure Al_2O_3.
- Increasing the Al_2O_3 volume content in the composite, increase the chemical reactivity at 1500°C.

SEM - Composites characterization

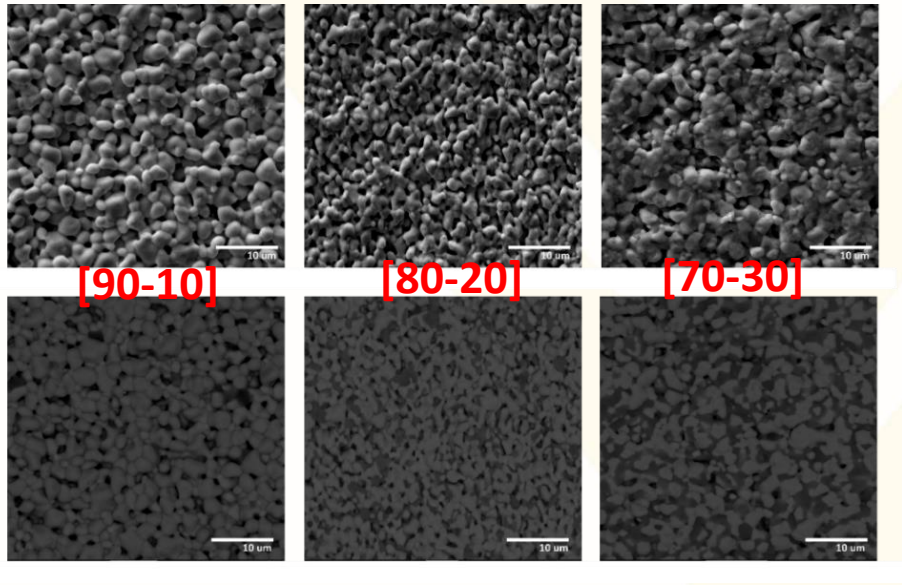

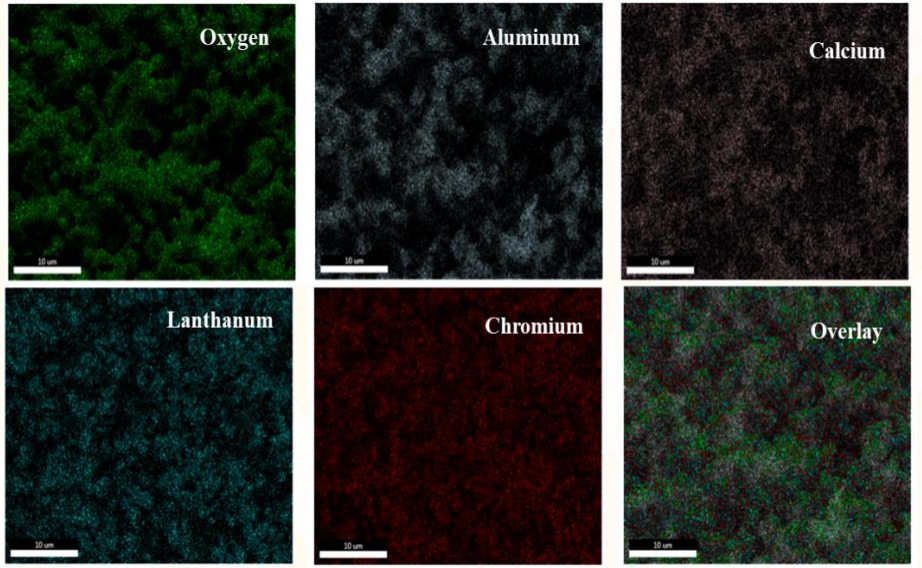

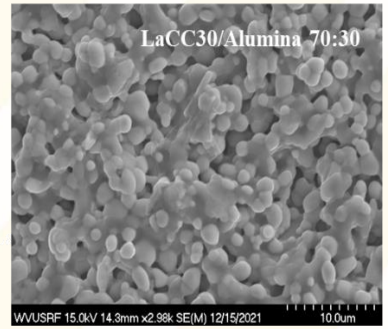

- At 10 vol% of Al_2O_3 there is not connectivity between grains indicating the formation of a (3-0) composite.
- At 20 vol% and 30 vol% the connectivity of the grains is more notable, indicating the formation of (3-3) composites.
- These results demonstrated that the degree of percolation of Al_2O_3, $LaAlO_3$ and $Ca_2Al_2O_5$ grain size increased by increasing Al_2O_3 content from 10 to 30 vol%.